



## Exoelectrogenic anaerobic granular sludge for simultaneous electricity generation and wastewater treatment

Zhao, Nannan; Treu, Laura; Angelidaki, Irini; Zhang, Yifeng

*Published in:*  
Environmental Science and Technology

*Link to article, DOI:*  
[10.1021/acs.est.9b03395](https://doi.org/10.1021/acs.est.9b03395)

*Publication date:*  
2019

*Document Version*  
Peer reviewed version

[Link back to DTU Orbit](#)

*Citation (APA):*  
Zhao, N., Treu, L., Angelidaki, I., & Zhang, Y. (2019). Exoelectrogenic anaerobic granular sludge for simultaneous electricity generation and wastewater treatment. *Environmental Science and Technology*, 53(20), 12130-12140. <https://doi.org/10.1021/acs.est.9b03395>

---

### General rights

Copyright and moral rights for the publications made accessible in the public portal are retained by the authors and/or other copyright owners and it is a condition of accessing publications that users recognise and abide by the legal requirements associated with these rights.

- Users may download and print one copy of any publication from the public portal for the purpose of private study or research.
- You may not further distribute the material or use it for any profit-making activity or commercial gain
- You may freely distribute the URL identifying the publication in the public portal

If you believe that this document breaches copyright please contact us providing details, and we will remove access to the work immediately and investigate your claim.

## Exoelectrogenic anaerobic granular sludge for simultaneous electricity generation and wastewater treatment

Nannan Zhao, Laura Treu, Irini Angelidaki, and Yifeng Zhang

*Environ. Sci. Technol.*, **Just Accepted Manuscript** • DOI: 10.1021/acs.est.9b03395 • Publication Date (Web): 11 Sep 2019

Downloaded from [pubs.acs.org](https://pubs.acs.org) on September 11, 2019

### Just Accepted

“Just Accepted” manuscripts have been peer-reviewed and accepted for publication. They are posted online prior to technical editing, formatting for publication and author proofing. The American Chemical Society provides “Just Accepted” as a service to the research community to expedite the dissemination of scientific material as soon as possible after acceptance. “Just Accepted” manuscripts appear in full in PDF format accompanied by an HTML abstract. “Just Accepted” manuscripts have been fully peer reviewed, but should not be considered the official version of record. They are citable by the Digital Object Identifier (DOI®). “Just Accepted” is an optional service offered to authors. Therefore, the “Just Accepted” Web site may not include all articles that will be published in the journal. After a manuscript is technically edited and formatted, it will be removed from the “Just Accepted” Web site and published as an ASAP article. Note that technical editing may introduce minor changes to the manuscript text and/or graphics which could affect content, and all legal disclaimers and ethical guidelines that apply to the journal pertain. ACS cannot be held responsible for errors or consequences arising from the use of information contained in these “Just Accepted” manuscripts.

1 **Exoelectrogenic anaerobic granular sludge**  
2 **for simultaneous electricity generation and**  
3 **wastewater treatment**

4 *Nannan Zhao<sup>1,2</sup>, Laura Treu<sup>1</sup>, Irimi Angelidaki<sup>1</sup>, Yifeng Zhang<sup>1\*</sup>*

5 <sup>1</sup>Department of Environmental Engineering, Technical University of Denmark, DK-2800  
6 Lyngby, Denmark.

7 <sup>2</sup>College of Life Sciences, Zhejiang Sci-Tech University, 310018 Hangzhou, PR China.

8

9

10

11

12

13

14

15

16

---

\*Corresponding author, Tel.: +45 45251410; fax: +45 45932850.

E-mail address: yifz@env.dtu.dk; yifzmf@gmail.com (Yifeng Zhang)

17 **Abstract**

18 Thick and electroactive biofilm is the key for successful development of microbial  
19 electrochemical technologies and systems (METs). In this study, intact anaerobic granular  
20 sludge (AGS), which are spherical and dense microbial associations, was successfully  
21 demonstrated as novel and efficient biocatalysts in METs such as microbial fuel cell  
22 (MFC). Three different strategies were explored to shift the microbial composition of AGS  
23 from methanogenic into exoelectrogenic microbes, including varying external resistance,  
24 organic loading, and manipulating anode potential. Among other strategies, only with  
25 positive anode potential, AGS was successfully shifted from methanogenic to  
26 exoelectrogenic conditions, as indicated by the significantly high current response (10.32  
27 A/m<sup>2</sup>) and 100% removal of organic carbon from wastewater. Moreover, AGS bioanode  
28 showed no significant decrease in current generation and organic removal at pH 5,  
29 indicating good tolerance of AGS to acidic conditions. Finally, 16S rRNA sequencing  
30 revealed the enrichment of exoelectrogens and inhibition of methanogens in the microbial  
31 community of AGS after anode potential control. This study provides a proof-in-concept  
32 of extracting electrical energy from organic wastes by exoelectrogenic AGS along with  
33 simultaneous wastewater treatment, and meanwhile opens up a new paradigm to create  
34 efficient and cost-effective exoelectrogenic biocatalyst for boosting the industrial  
35 application of METs.

36 **Keywords:** Anaerobic granular sludge; Exoelectrogenic biocatalyst; Electric energy; 16S  
37 rRNA analysis; Wastewater treatment.

38

## 39 **Introduction**

40 Growing concerns over the intensive energy consumption for conventional wastewater  
41 treatment technologies has boosted interest in the development of energy-neutral treatment  
42 technologies<sup>1</sup>. Microbial electrochemical technologies and systems (METs) has shown  
43 promising potential in several applications spanning from renewable electricity production  
44 to biochemical and bioproducts production by using the electrons derived from waste  
45 organic matters by bacteria to perform dedicated reduction reaction<sup>2-4</sup>. Though promising,  
46 MFC technologies are still encountering a long-standing challenge to develop thick and  
47 efficient electroactive biofilm on the anode electrode. On the one hand, the limited biomass  
48 content and retention in biofilm would lead to the low capacity for organic carbon removal  
49 compared to conventional biotechnologies, and thus, extra post-treatment processes are  
50 always required<sup>5, 6</sup>, which would greatly increase the operational and maintenance cost. On  
51 the other hand, MFC reactors which rely on thin anodic biofilm can't produce substantial  
52 quantities of power to offset the practical energy demands for wastewater treatment<sup>7, 8</sup>.  
53 Thus, the conventional ways of fabricating electroactive biocatalysts (as biofilm) on the  
54 anode do limit the wide application of MFC technology for wastewater treatment and  
55 energy generation<sup>6, 9</sup>.

56 In the past decades, anaerobic granular sludge (AGS), as aggregates of microorganism, is  
57 popular among anaerobic biocatalysts for simultaneous bioenergy production (i.e., biogas  
58 through anaerobic digestion) and wastewater treatment, due to its high organic removal  
59 capacity and good tolerance to extreme conditions (e.g., toxic compounds and acidic  
60 shocks)<sup>10-12</sup>. In a previous MFC study<sup>13</sup>, homogeneous bacterial suspension, derived from  
61 grinded AGS using a mortar and pestle followed by filtration (0.25-mm pore size sieve),

62 has even been demonstrated as efficient inoculum for cultivating anodic biofilm. Thus,  
63 AGS could be a potential habitat of exoelectrogenic bacteria, in addition to methanogens.  
64 More recently, it has been found that the whole microbial aggregates can be electroactive  
65 if direct interspecies electron transfer occurs among the diverse microbial consortia<sup>14, 15</sup>.  
66 Considering the essential properties of AGS with dense microbes, special channel  
67 morphology and potential conductivity, it is reasonable to hypothesize that intact AGS  
68 could function as an effective biocatalyst for an MFC if electroactive bacteria are enriched  
69 inside of granule. To date, intact AGS has never been tested as electroactive biocatalyst in  
70 the field of METs. Integration of intact AGS into anode could address the key challenge of  
71 MFC and greatly boost its capacity for electricity generation and wastewater treatment.  
72 Such combination could further strength the advantages of MFC over conventional  
73 anaerobic treatment processes, in addition to the inherent merits of mild operating  
74 conditions, high removal and energy efficiency for low strength wastewater, and easy use  
75 and transport of end product (electricity in this case)<sup>16, 17</sup>.

76 In this context, switching intact AGS from methanogenic to exoelectrogenic is a key to  
77 achieve a successful integration. Thus, in this study, intact AGS was for the first time  
78 manipulated and explored as biocatalyst in MFC for wastewater treatment and  
79 bioelectricity generation. Several strategies to transform the intact AGS from  
80 methanogenic to exoelectrogenic, were employed, and the outcomes were evaluated in  
81 terms of organic removal, current response, and coulombic efficiency. Finally, the  
82 microbial dynamics during manipulation of anode potential and microbial composition at  
83 different sites of anode electrode were analyzed. To the best of our knowledge, it is the first  
84 time to investigate the feasibility of tailoring intact granular sludge as biocatalyst for

85 bioelectricity generation, which offers new insights in development of viable and  
86 sustainable technology for cost-effective and efficient wastewater treatment.

## 87 **Materials and methods**

### 88 **MFC set up**

89 An MFC, made of nonconductive polycarbonate plates was constructed. The anode and  
90 cathode chambers with the same dimension size ( $4 \times 5 \times 5$  cm) were separated by a cation  
91 exchange membrane (CEM, CMI 7000, Membrane international, NJ). Rubbers and screws  
92 were used to tighten the reactor to avoid leakage. The anode electrode was made of a carbon  
93 fiber brush wound into two twisted titanium wires (5.0 cm diameter, 5.0 cm length, Mill-  
94 Rose, USA), which were heated at 450 °C for 15 minutes before use as reported  
95 previously<sup>18</sup>. A reference electrode of Ag/AgCl electrode (+0.197 V vs SHE) was placed  
96 ~ 0.3 cm close to the anode for accurate control of anode potential. The anodic chamber  
97 was filled with 80 g wet AGS, which was collected from a mesophilic upflow anaerobic  
98 sludge blanket reactor fed with potato wastewater (Colsen, Netherland). A stainless-steel  
99 mesh was used to avoid the washing out of AGS and possible blocking issues. The total  
100 volume of anode chamber was 100 ml, while the working volume was 50 ml. An external  
101 recirculation bottle (filled with 500 ml synthetic wastewater) was connected to anode  
102 chamber with a recirculation flow rate of 50 ml/min. To maintain a sufficient mixing, the  
103 recirculation bottle was stirred at 400 rpm. A titanium woven wire mesh (4×4 cm, 0.15 mm  
104 aperture, William Gregor Limited, London) coated with 0.5 mg/cm<sup>2</sup> Pt was used as cathode  
105 electrode. In closed circuit, the anode and cathode electrodes were connected through an  
106 external resistance (1000 Ω, unless otherwise stated). During anode potential control by

107 potentiostat (Ivium-n-Stat, Ivium Technologies, Eindhoven, The Netherlands), three-  
108 electrode cell mode was adopted; anode as working electrode, cathode as counter electrode  
109 and Ag/AgCl as reference electrode.

#### 110 **Inoculation and operational strategies**

111 AGS was directly used as the inoculum for MFC start-up. The synthetic wastewater  
112 contained (in g/L of distilled water): sodium acetate, 1 (unless otherwise stated); NH<sub>4</sub>Cl,  
113 0.31; NaH<sub>2</sub>PO<sub>4</sub>·H<sub>2</sub>O, 2.69; Na<sub>2</sub>HPO<sub>4</sub>, 4.33; KCl, 0.13; 12.5 ml mineral solution and 12.5  
114 ml vitamin solution as described before<sup>19</sup>. The final pH of synthetic wastewater always  
115 kept  $7.0 \pm 0.2$ . The anode chamber and external bottle was filled with the aforementioned  
116 synthetic wastewater, reaching a total volume of 550 ml. The cathode chamber was filled  
117 with 100 ml ferricyanide solution (50 mM, pH 7) to exclude the instability of cathodic  
118 reaction. The catholyte was 50 mM phosphate buffer solution containing 50 mM  
119 ferricyanide.

120 Multiple reactors including duplicate set-ups have been operated for the tests according to  
121 different purposes. Three strategies were employed successively in the same reactor. As  
122 summarized in Table S1 in supporting information, strategy 1 referred to the effect of  
123 external resistance on MFC performance under closed circuit. During strategy 1 operation,  
124 the sodium acetate concentration was controlled at 1500 mg/L. Thereafter, the influence of  
125 different organic loading (1000, 1500 and 3000 mg/L) on system performance was  
126 evaluated in strategy 2, during which the resistance was selected as 10  $\Omega$ . Subsequently, in  
127 strategy 3, MFC was connected to the potentiostat and chronoamperometry measurement  
128 was used to control anode potential at +20 mV (VS Ag/AgCl). During strategy 3, the



129 sodium acetate level was 1000 mg/L. Sequentially, to evaluate the persistence of positive  
130 effect by controlling anode potential, MFC was connected in a closed circuit with 10  $\Omega$   
131 resistance, and fed with 1000 mg/L sodium acetate. Afterwards, the AGS were removed  
132 out of the anode chamber to evaluate the functions of AGS, denoted as Control 1. The  
133 cultivated AGS were transferred into another identical MFC with a completely new anode  
134 to explore the current generation of the removed AGS, denoted as Control 2. The  
135 transferring process was performed in an anaerobic box. The operational parameters (1000  
136 mg/L sodium acetate and 10  $\Omega$  resistance) were employed for Control 1 and Control 2. At  
137 the end, to evaluate the robust resistance to low pH conditions, same AGS were placed  
138 back to the anode chamber and operated under different initial wastewater pH varying from  
139 5 to 7. For comparison of AGS powered MFC with conventional MFC inoculated with  
140 domestic wastewater, one set of MFC reactors with same configuration was constructed  
141 (Control 3) and inoculated with domestic wastewater obtained from primary clarifier at  
142 Lundtofte Wastewater Treatment Plant (Lyngby, Denmark). For all the reactors, at the  
143 beginning of each batch, anode chamber and recirculation bottle was flushed with pure N<sub>2</sub>  
144 for 10 minutes to keep anaerobic conditions.

#### 145 **Analytical methods and calculations**

146 During strategy 1 and 2, the voltage across an external resistance was recorded by a digital  
147 multimeter (model 2700, Keithley Instruments, Inc.; Cleveland, OH) every 30 minutes.  
148 Current was calculated according to ohm's law ( $I=U/R$ ). Current density was normalized  
149 by the projected cathode area (16 cm<sup>2</sup>). During strategy 3, the current response was  
150 recorded by the potentiostat every 1 min. Coulombic efficiency (CE) was calculated as

151  $CE = \frac{C_t}{C_{th}} \times 100\%$ , where  $C_t$  was the total coulombs calculated by integrating current  
152 response with time, calculated as  $C_t = \int Idt$ ,  $C_{th}$  was the theoretical amount of coulombs  
153 based on the COD degradation, calculated as  $C_{th} = \frac{Fb\Delta COD}{M}$ , where F is Faraday's  
154 constant ( $96485 \text{ C mol}^{-1} \text{ e}^-$ ), b is 4 referring to the transferred electrons per mole of oxygen,  
155 M is 32 representing the molecular weights of oxygen,  $\Delta COD$  is the removed COD amounts  
156 (unit gram)<sup>20</sup>.

157 Total chemical oxygen demand (TCOD) was measured according to the standard method  
158 (APHA, 1999). COD removal rates were fitted assuming a first-order kinetic reaction with  
159 respect to substrate concentrations, and calculated according to the following equation:

160 
$$\ln \frac{COD_t}{COD_0} = -kt \quad \text{Eq (1)}$$

161 where  $COD_0$  is the initial COD concentration,  $COD_t$  is the COD concentration at time t,  
162 and k is the first-order kinetic rate coefficient. The coefficient k at varied pH was calculated  
163 and compared in section 3.2, in order to distinguish the optimal pH regarding to the fastest  
164 carbon utilization.

165 Acetate was measured via a GC with FID detection (Agilent 6890). The sample pH was  
166 immediately measured by using A PHM 210 pH meter (Radiometer). Produced gas was  
167 collected by connecting a gasbag to the headspace of recirculation bottle. The volume was  
168 measured by a 100 ml syringe.  $\text{CO}_2$  and  $\text{CH}_4$  were analyzed by a GC-TCD fitted with  
169 paralleled column of  $1.1 \text{ m} \times 3/16$  'Molsieve 137 and  $0.7 \text{ m} \times 1/4$ ' with  $\text{H}_2$  as the carrier  
170 gas (MGC 82-12, Microlab A/S, Denmark), and  $\text{H}_2$  was determined by a GC-TCD fitted

171 with a 4.5 m × 3 mms-m stainless column packed with Molsieve SA (10/80), as previously  
172 described<sup>21</sup>.

173 Mastersizer 2000 (Malvern Instruments, UK) was employed to measure the particle size  
174 distribution of the raw AGS and cultivated AGS after strategy 3. Scanning electron  
175 microscopy (SEM - FEI Quanta 200 ESEM FEG equipped with energy dispersion  
176 spectroscopy, EDS - Oxford) was used for the observation of AGS morphology. For  
177 morphological characterization, the raw AGS and AGS after strategy 3 were sampled,  
178 washed with phosphorus buffer solution (50 mM, pH 7) and fixed by soaking into 4%  
179 formaldehyde for 24 hours at 4 °C. Subsequently, the samples were washed by gradient  
180 25%, 50%, 75%, 90%, 95%, and 100% ethanol/distilled water solutions successively.  
181 Afterwards, samples were freeze-dried for overnight to get the powder specimens. The  
182 specimens were coated with a gold thin layer (Quorum sputter coater, UK) and observed  
183 by SEM-EDS at 3.0 kV.

#### 184 **Microbial community analysis**

185 To characterize changes in microbial community before and after operation, the raw  
186 granules, and the enriched granules and anodic biofilm after strategy 3 were all collected  
187 by using sterilized scalpel or spoon as previously described<sup>22</sup>. Granules were sampled at  
188 either in the direct vicinity, or further away from the anode. All the samples were collected  
189 in triplicate except the biofilm which was sampled in duplicate. Total DNA extraction was  
190 performed using PowerSoil DNA Isolation Kit (MoBio PowerSoil, Carlsbad, CA, USA).  
191 Total genomic DNA amplification using universal primers 515F/806R was conducted on

192 V4 hypervariable region of 16S rRNA gene, and amplicons were sequenced by Illumina  
193 MiSeq desktop sequencer (Ramaciotti Centre for Genomics, Kensington, Australia).

194 Raw data was deposited in the Sequence Read Archive database  
195 (<https://www.ncbi.nlm.nih.gov/sra>) under the accession number PRJNA485399. OTU  
196 clustering and taxonomy identification were performed using microbial genomics module  
197 plug of CLC Workbench software (V.8.0.2, QIAGEN) as previously described<sup>23</sup>. OTU was  
198 chosen to represent the Alpha diversity, while Principal Component Analysis (PCA)  
199 performed by STAMP software<sup>24</sup> was selected to represent Beta diversity. The taxonomical  
200 assignments of the selected interesting OTUs (relative abundance over 0.5%) was  
201 performed including a manual comparison of CLC results with 16S ribosomal RNA  
202 sequences (Bacteria and Archaea) database at the National Center for Biotechnology  
203 Information (NCBI) by using BLAST<sup>23</sup>. Microbial relative abundance and folds change  
204 were visualized in heat maps using Multi experiment viewer software (MeV 4.9.0).  
205 Statistics regarding to the significant differences in microbial communities were identified  
206 by t-test in STAMP software.

## 207 **Results and discussion**

### 208 **Different strategies to enhance the electroactivity of AGS for bioelectricity generation** 209 **and wastewater treatment**

#### 210 *Impact of external resistance*

211 Figure 1 is here.

212 The strategy of varying external resistance was first applied to the MFC reactor inoculated  
213 with AGS. The current density, as representative of electricity generation, showed a  
214 different behavior with different resistances (Figure 1A). When external resistance was  
215 changed from 1000 to 10  $\Omega$ , 14 fold increase of maximum current density (from 0.41 to  
216 5.84 A/m<sup>2</sup>) was observed at the same acetate level (1500 mg/L). The trend of current  
217 generation at different external resistances was consistent with previous studies<sup>25, 26</sup>.  
218 During the same period (Figure 1B), The COD removal was greatly improved (from 67%  
219 to 87%) when MFC was switched from 1000 to 10  $\Omega$ . The higher COD removal rate at 10  
220  $\Omega$  indicated that the substrate oxidation rate was enhanced when subjected to lower  
221 resistance. Regarding to the biogas production rate and methane yield, it was noticeable  
222 that the methane production was significantly increased at 10  $\Omega$  (Figure 1C). The result  
223 showed that the increase of COD removal after changing resistance to 10  $\Omega$  was partly due  
224 to the anaerobic methanation. The results were different from the previous studies that  
225 methanogens activity was inhibited at lower resistance<sup>27-29</sup>. In this study, the AGS was  
226 originally cultivated for biomethanation which was different from previous MFC studies.  
227 In addition, decreasing external resistance could be an effective way to enrich  
228 exoelectrogens, but it may also facilitate interspecies electron transfer between  
229 exoelectrogens and methanogens as reported previously<sup>30</sup>. There was no significant  
230 difference in anodic potential (around -500 mV) and pH (approx. pH 7) during the  
231 operation with two different external resistances (data not shown). The influence of pH in  
232 the methanogenic activity could be neglected. Thus, strategy 1 referred to changing  
233 resistance was not an effective way to inhibit methanogenic activity. Considering the  
234 enhanced electricity production, R-10  $\Omega$  was selected for the following experiments.

### 235 ***Impact of substrate concentration***

236 According to the previous study<sup>31</sup>, the methanogens activity could be manipulated by  
237 organic loading. Therefore, as strategy 2, the acetate concentrations ranging over 1000,  
238 1500 and 3000 mg/L was applied consecutively. As shown in Figure 1A, the current  
239 response significantly decreased when the acetate concentration increased from 1000 to  
240 1500 or 3000 mg/L. It suggested the exoelectrogens weren't activated by elevated organic  
241 loading. The electricity production was inhibited by increasing organic loading, as the  
242 current density at 1000 mg/L was the highest among all conditions. From the COD removal  
243 performance, it was clearly observed that COD removal rate was greatly enhanced with  
244 elevated acetate concentrations. The average COD removal rate for 1000, 1500 and 3000  
245 mg/L was 70.99, 110.59 and 360.60 mg/L/d, respectively. The COD removal was probably  
246 contributed by (1) acetate oxidation by exoelectrogens; (2) acetate oxidation by  
247 methanogens; (3) acetate oxidation by aerobic microbes. On one hand, from the  
248 aforementioned current response (Figure 1A), it was clearly observed that current density  
249 didn't increase dramatically with increasing of organic loading, which indicated that the  
250 contribution of exoelectrogens to acetate oxidation wasn't enhanced with improved carbon  
251 loading. On the other hand, due to the anolyte was flushed with nitrogen gas before starting  
252 each test, the contribution by aerobic oxidation could be limited. Thus, the only possible  
253 reason would be due to the activity of methanogens. To confirm our speculation, the biogas  
254 production rate and methane yield were further analysed. As depicted in Figure 1C, the  
255 higher acetate concentration, the faster methane production rate was observed, suggesting  
256 the active methanogenesis process at elevated acetate concentration. Also, the methane  
257 yield increased accordingly, which indicated the unsuccessful inhibition of methanogens

258 activity by improving organic loading. It was noticeable that in all cases, methane contents  
259 always kept almost ten times higher than carbon dioxide. This could be due to its high  
260 solubility of CO<sub>2</sub>. Recirculation of liquid was applied in the anode, which may promote the  
261 dissolution of CO<sub>2</sub>. Overall, the above results demonstrated that the acetate concentration  
262 of 1000 mg/L was good to obtain a superior electricity generation, and the substrate  
263 concentration was not the contributing for turning methanogenic AGS into electrogenic.

#### 264 ***Impact of anodic potential***

265 Figure 2 is here.

266 In addition to external resistance and organic loading, the anode potential has been reported  
267 to impact microbial community structure and electrochemical performance<sup>29, 32</sup>. Therefore,  
268 controlling anode potential at +20 mV (VS Ag/AgCl) as the third strategy was employed.  
269 Clearly, during the period of anode potential control, the acetate was degraded rapidly in 5  
270 days (Figure 2B). In fact, after 3 days, the acetate concentration already decreased from  
271 800 to 33 mg/L, resulting in 96% removal. Correspondingly, the peak current density  
272 increased significantly to 10.32 A/m<sup>2</sup> (Figure 2A). The high current response with fast  
273 acetate degradation indicated that anode potential motivated the exoelectrogenic reactions  
274 other than methanogenic. On the one hand, positive anode potential meant more energy to  
275 support electroactive bacterial growth. It was reported that at relatively higher anode  
276 potential, exoelectrogens can theoretically gain more energy for their growth and  
277 maintenance<sup>33, 34</sup>, according to:

$$278 \quad \Delta G^{0'} = -nF(E_{anode} - E_{donor}^{0'})$$

279 where  $\Delta G^{0'}$  is the Gibbs free energy change at standard conditions (pH 7 and 25°C),  $n$  is  
280 the number of electrons transferred,  $F$  is Faraday's constant (96485 C mol<sup>-1</sup> e<sup>-</sup>),  $E_{anode}$  is  
281 the anode potential,  $E_{donor}^{0'}$  is the standard biological redox potential of electron donor. On  
282 the other hand, positive anode potential may affect the electron transfer kinetics and attract  
283 bacteria to move towards the electrode to form a thick biofilm<sup>35</sup>. Therefore, when the anode  
284 potential was increased from -550 mV (measured anode potential at closed-circuit) to +20  
285 mV, both of the carbon removal and current generation were greatly enhanced. To confirm  
286 the inhibited methanogenic activity at high anode potential, biogas production rate and  
287 methane yield were analysed. As shown in Figure 2C, methane yield almost decreased to  
288 0, which indicated that the methanogenic activity was fully suppressed at high anode  
289 potential. Furthermore, it was reported that the amounts of proteins (i.e. OmcA), which are  
290 responsible for extracellular electron transfer, increased with elevating anodic potential<sup>35</sup>.  
291 More direct electron transfer-related protein at positive potential helped to stimulate an  
292 electroactive-biofilm formation<sup>35</sup>.

293 To examine the persistence of this strategy for electroactive bacteria enrichment, the  
294 reactor was subsequently switched to MFC mode (without potential control) again. It was  
295 shown that the peak current density increased from 3.30 (before potential control) to 6.41  
296 A/m<sup>2</sup> (after potential control) when it was fed with 1000 mg/L acetate (Figure 2A). The  
297 acetate removal efficiency increased from 50% (9 days) to 100% (8 days), indicating  
298 effectiveness of anode potential control on enrichment of exoelectrogens. The pH was quite  
299 stable (around pH 7 during each batch run, data not shown) before and after potential  
300 control. The contribution of capacitive effect to the high current generation after potential  
301 control could be neglected, since the maximum stable current generation lasted for a few



302 hours while discharging behaviour is normally around few seconds to minutes. To further  
303 explore the contribution of AGS in electricity generation and carbon removal, the  
304 performance of both MFC after removing AGS from anode chamber (Control 1) and new  
305 MFC anode with removed AGS (Control 2) were investigated, respectively. In control 1,  
306 the peak current density immediately decreased from 6.59 to 0.52 A/m<sup>2</sup>, suggesting that  
307 the AGS was partially involved in electron transfer. Accordingly, the acetate concentration  
308 decreased from 731 to 166 mg/L after 7 days, resulting in 77% acetate removal. Since no  
309 methane was produced in control 1, the contribution of methanogens to acetate removal  
310 could be excluded. The current response and carbon removal observed in control 1 could  
311 be due to small amount of residual AGS on anode since it is impossible to remove all AGS  
312 from the anode. As shown in Figure S1, a completely new anode with cultivated AGS  
313 produced a maximum current density of 1.11 A/m<sup>2</sup> after 1 day, which was higher than  
314 control 1. But it didn't recover to the level observed before moving. The results of two  
315 controls indicated that both AGS and formed biofilm on electrode played a  
316 vital/cooperative role for the current generation. Even the AGS was exoelectrogenic, the  
317 last step of electron transfer from bulk solution to solid electrode may still require an  
318 electroactive biofilm as electron conduit.

319 To short conclude, the above results indicated that anode potential controlled at +20 mV is  
320 effective to facilitate electroactive species growth and electron transfer in AGS.  
321 Methanogens are well known strict anaerobes i.e. they require very low potential to grow  
322 (<-300 mV). Therefore, exoelectrogens could dominate and got exclusively the chance to  
323 use acetate as substrate.

324 **Acid resistance**

325 Figure 3 is here.

326 In the previous studies, the most common inoculum for MFC electroactive biofilm  
327 enrichment was domestic wastewater, which was either attached on anode or suspended in  
328 liquid<sup>36, 37</sup>. Comparatively, the AGS with diverse microbes and intrinsic granular structure  
329 was used as inoculum in our work. It was previously reported that wastewater pH would  
330 significantly affect MFC performance<sup>29</sup>. Thus, in this section, the effect of pH shock on the  
331 electrogenic capacity of the enriched AGS anode was investigated. Figure S2 depicts  
332 acetate removal rates which showed good agreement with the current output at different  
333 pH ranging over 5 to 7 (Figure S2). The maximum current density at each condition was  
334 shown in Figure 3. The highest maximum current density ( $5.21 \text{ A/m}^2$ ) was observed at pH  
335 7 in AGS-MFC. When pH was decreased from 7 to 5, the ability of electron production  
336 was significantly deteriorated for both reactors. It was reported that exoelectrogens  
337 couldn't survive in the acidic environment when pH was lower than 5.5<sup>38</sup>. Although both  
338 of reactors were negatively affected by the acid pH, AGS-MFC showed a relatively  
339 stronger resistance to low pH compared to typical MFC inoculated with wastewater.  
340 Assuming first-order kinetics, the rate coefficient was calculated according to Eq. (1), as  
341 displayed in Figure 3. In both reactors, the rate coefficient showed a similar trend to pH  
342 variations. The highest rate of  $0.35 \text{ d}^{-1}$  was obtained at pH 7 in AGS-MFC. In AGS-MFC,  
343 when pH was decreased from 7 to 5, the rate coefficient decreased correspondingly from  
344  $0.35$  to  $0.20 \text{ d}^{-1}$ , indicating diminished substrate degradation at acidic environment.  
345 Similarly, for control MFC, the rate coefficient decreased from  $0.20$  to  $0.12 \text{ d}^{-1}$ . The rate  
346 coefficient at pH 5 in AGS-MFC was even close to the value of control reactor at pH 7,

347 meaning a superior performance of acetate oxidative reaction in AGS-MFC even at  
348 unfavourable pH conditions. Clearly, neutral pH conditions proved to be the optimal  
349 environment for the exoelectrogenic bacteria. AGS inoculated MFC would have better  
350 resistance considering that the biofilm from AGS might become even thicker during long-  
351 term operation.

### 352 **Morphological characteristics and elemental composition of AGS**

353 Figure 4 is here.

354 The morphological image of single AGS taken after strategy 3 was depicted in Figure 4.  
355 As shown in Figure 4A, an AGS has a spherical rough surface and macroporous carbon  
356 architecture. A zoomed in image of the surface is shown in Figure 4B, in which the entire  
357 surface of AGS was covered with compact rod-shaped bacterial cells. The porous structure  
358 and rough surface would be beneficial for microbial growth and biofilm formation<sup>39</sup>. In  
359 addition to the excellent porous structure, granules exhibit good mechanical strength for  
360 microbes to resist the changes of surrounded environments (such as extreme pH or organic  
361 loading shock) compared to the conventional flocs or biofilm<sup>12, 40</sup>. High-resolution of SEM  
362 images of AGS channels (Figure 4C) demonstrated deep channels of ca. 1  $\mu\text{m}$  diameter,  
363 with rod-shaped bacteria aligned on the channel sides. It revealed that the bacterial cells  
364 were densely adhered not only to AGS surface, but also interior sections of AGS, indicating  
365 the porous structure of AGS permitted sufficient substrate exchange from outside to inside  
366 to support internal biofilm growth<sup>41</sup>. All of these attractive properties (the porous structure,  
367 rough surface and dense microbes) enabled AGS as an ideal inoculum candidate for MFC  
368 exoelectrogens enrichment.

369 According to the EDS results (Figure 4D), the raw AGS contained high levels of carbon  
370 (53%) and oxygen (32%), and small amounts of minerals such as silicon, calcium and other  
371 traditional metals including iron. These minerals were reported as the main skeleton of  
372 granular structure, and may be involved in the electrical double layer formation of AGS as  
373 reported before<sup>42, 43</sup>. After strategy 3, the cultivated AGS contained higher amounts of  
374 carbon, which could be assigned to the increasing biomass contents. The low deviation  
375 suggested a homogeneous mineralized granular structure. To get further information of the  
376 granule size, Mastersizer 2000 was used to measure the particle size distribution (Figure  
377 4E). It was found the mean diameter based on the volume weighted was significantly  
378 increased from 122 (raw AGS) to 760  $\mu\text{m}$  (cultivated AGS). It means over 50% granules  
379 had the diameter of 760  $\mu\text{m}$  after anode potential control. The bigger size demonstrated  
380 that granulation of AGS was enhanced after being shifted from methanogenic to  
381 electrogenic condition<sup>44</sup>. This is also consistent with the higher energy gain of bacteria at  
382 higher anodic potential which would inevitably result in higher cell biomass.

### 383 **The influence of anode potential manipulation in microbial community dynamics**

384 After the selection and comparison of three strategies, strategy 3 (anode potential) was  
385 demonstrated to be the most effective to inhibit methane production and improve current  
386 generation. To gain an insight into microbial communities residing in granules and in  
387 biofilm of carbon brush, 16S rRNA gene analysis was employed.

388 According to alpha diversity results shown in Figure S3 (Supporting Information), an  
389 increase in microbial diversity (represented as OTU) regardless of sampling position was  
390 observed after potential control. The results indicate that a more diverse microbiome was

391 enriched after a positive anode potential. Beta diversity shown in Figure S4A demonstrated  
392 a distinct microbial dynamic change before and after anode potential control. A dramatic  
393 change was found between raw granules and enriched granules/biofilms after strategy 3  
394 based on the principal percentage (PC1 and PC2) (Figure S4A). When taking further  
395 analysis of PC3, AGS taken from different positions (close and far from anode) were also  
396 different from each other in microbial community compositions. Same distinct difference  
397 was observed between granules and anodic biofilm. The above results were in agreement  
398 with previous findings that the anode potential significantly affected the microbiome  
399 clustering in anode<sup>34</sup>.

400 Figure 5 is here.

401 High throughput 16S RNA amplicon sequencing was used to analyze the microbial  
402 dynamics in AGS and attached anodic biofilm, and the relative abundance of taxa over 0.5%  
403 is illustrated in Figure 5A. The vast majority of raw AGS microbial community was  
404 composed of 90% bacteria (based on the average relative abundance). *Bacteroidetes* (23%),  
405 *Firmicutes* (23%), *Proteobacteria* (12%), followed by *Synergistetes* (9%), and others  
406 (23%), were the most dominant phyla (Figure S5). The microbial composition in raw AGS  
407 was in agreement of common mesophilic AGS as reported before<sup>45</sup>. *Bacteroidetes*,  
408 *Firmicutes* and *Proteobacteria* has always been detected in MFC, which were supposed to  
409 be responsible for electricity generation<sup>32, 46</sup>. Thus, the raw AGS probably already  
410 contained electroactive bacteria in the innate microbial community, which could enable its  
411 utilization as biocatalyst in an MFC.

412 To get an insight into how the microbial community composition in MFC, the changes  
413 between the raw and enriched AGS after manipulating anode potential were compared. The

414 results are shown in Figure 5B. As illustrated, in a cluster of taxa (Figure 5B, Group 1),  
415 increasing significantly in relative abundance after manipulating anode potential was  
416 mainly composed by exoelectrogenic bacteria. For example, *Synergistaceae* spp. (5 and 6)  
417 increased from 0.2% to over 10% of relative abundance in both the granules and biofilm,  
418 indicating that the proliferation of species belonging to *Synergistaceae* was due to the  
419 improved anode potential. The family *Synergistaceae* was often found in MFC anode<sup>47</sup>. It  
420 was noticeable that the strain of *Arcobacter butzleri* spp. (16 and 8), known as  
421 exoelectrogens<sup>48</sup>, appeared after the potential control (accounting for 6.5% of relative  
422 abundance in the biofilm sample), strongly supported the enrichment of exoelectrogens.  
423 Also, *Desulfurmonadales* spp. appeared after improving anode potential, suggesting a  
424 strong correlation to the potential change. The *Desulfurmonadales* spp. (22 and 65) showed  
425 a 97% similarity to *Pelobacter propionicus* and *Geobacter chappellei*. *Pelobacter*  
426 *propionicus* was known as propionate producer from acetate, while no propionate was  
427 detected during the experiment. Therefore, the high similarity of the strain was very likely  
428 affiliated to *Geobacter chappellei*, which was reported as Fe(III) reducer<sup>49</sup>. Since iron-  
429 reducing bacteria are known to use electrode as electron acceptor, we deduce that  
430 *Desulfurmonadales* spp. represented by *Geobacter chappellei* may also have been involved  
431 in direct electron transfer to anode<sup>35</sup>. Furthermore, the strain affiliated to the family  
432 *Marinilabiliaceae* also increased in abundance, which has been previously found in MFC  
433 bioanode<sup>50</sup>. Interestingly, another known species *Methanobacterium beijingense* was  
434 dominant after improving anode potential. *M. beijingense* was known as hydrogenotrophic  
435 methanogens using H<sub>2</sub>/CO<sub>2</sub><sup>51</sup>. However, since no methane was detected, the species might  
436 contribute mainly to maintain the granular structure by acting as the nucleation center, as

437 described elsewhere<sup>52</sup>. It has to be mentioned that although the enrichment of  
438 exoelectrogens was demonstrated at positive anodic potential, the microbial community  
439 was different from the previous findings. The predominance of *Geobacter* species was  
440 typically reported for the acetate-fed MFCs<sup>53, 54</sup>, while in this study, the microbial  
441 community was more diverse with relatively fewer numbers of *Geobacter*. It was mainly  
442 due to the different inoculum sources<sup>53, 55</sup>. In this study, methanogenic AGS was used as  
443 the inoculum, while the domestic wastewater was often reported as the inoculum when  
444 *Geobacter* was the most abundant in the acetate-fed exoelectrogenic biofilms.

445 Comparatively, a cluster of taxa decreased significantly in relative abundance, which  
446 demonstrated that the transition from low anode potential (-550 mV) to high anode  
447 potential (+20 mV) created a hostile habitat to these taxa. More specifically, *Mesotoga*  
448 *infera*, which was involved in the conversion of acetate to H<sub>2</sub>/CO<sub>2</sub><sup>56</sup>, decreased from 9%  
449 close to 0%, indicating that this pathway was negatively affected by increasing anode  
450 potential. This was further supported by the undetectable H<sub>2</sub> throughout the whole  
451 experiment. Similarly, *Methanosaeta concilii*, known as acetoclastic methanogens that has  
452 ability of interspecies electron transfer with *Geobacter* species for CO<sub>2</sub> reduction into CH<sub>4</sub>,  
453 was diminished from 2.89% to 0.15%. This significant decrease indicated its inability to  
454 survive at high anode potential +20 mV. It has been reported that methanogens require a  
455 reductive environment where potential should be less than -527 mV (vs SHE) for its  
456 growth<sup>57</sup>. That simply explained the inhibition of methanogens at +20 mV. In a more recent  
457 work<sup>58</sup>, long-term open circuit was found preferable for the growth of methanogens in the  
458 cathode of acetogenic microbial electrosynthesis process, which implies the important role  
459 of circuit potential on the microbial communities on the electrode.

460 Furthermore, regarding the competition between exoelectrogens and methanogens, it has  
461 been proposed that a special structure of tightly packed aromatic amino acids enabled a  
462 long-range electron transport between *Geobacter* and *Methanosaeta*<sup>15</sup>. In the  
463 methanogenic aggregates, the known role of *Geobacter* species is converting acetate to  
464 CO<sub>2</sub> with electrons generating. Through the metallic-like conductive pili, electrons are  
465 released and flow to *Methanosaeta* for CO<sub>2</sub> reduction. The final electron sink is methane.  
466 The direct interspecies electron transfer way is broken down at positive anode potential  
467 since the *Methanosaeta* is not able to survive/active at high potentials<sup>59</sup>. Thus, when  
468 inserting a conductive electrode in the aggregates, the realised electrons from *Geobacter*  
469 metabolism would flow to the electrode instead of being involved in the methane  
470 production. In the exoelectrogenic condition, the solid electrode substitutes the  
471 *Methanosaeta* as the electron acceptor.

472 Figure 6 is here.

473 In order to elucidate the difference between the microbial community composition in  
474 anodic biofilm (taken from carbon brush), enriched AGS closed to anode electrode and  
475 enriched AGS far from anode, significant analysis based on the overall taxa were  
476 performed (Figure 6A and B). Distinct consortia were formed in enriched AGS samples  
477 and anodic biofilm. Compared to the anodic biofilm, a significant increase in relative  
478 abundance of 9 bacterial taxa was observed in the enriched AGS close to carbon brush.  
479 Particularly, well-known electrogenic bacteria such as *Marinilabiliaceae* spp.,  
480 *Anaerobineaceae* spp., and *Desulfovibrionales* spp. were found significantly increased in  
481 the AGS close to carbon brush. Besides, the significantly high abundance of *Synergistaceae*  
482 sp., which was previously demonstrated to be potentially electrogenic, was in accordance



483 with the electricity generation of Control 1 (MFC after removing granules). Comparatively,  
484 no significant difference was observed between AGS far from carbon brush and anodic  
485 biofilm, except one strain.

486 To get an additional insight into the difference between two AGS samples (one taken close  
487 to carbon brush and the other taken far from carbon brush), the statistical analysis was  
488 performed as well (Figure 6C). Clearly, 10 bacterial taxa were observed in significantly  
489 higher relative abundance in AGS close to carbon brush compared to the AGS far from  
490 carbon brush. The most significant increase was found in *Arcobacter butzleri*, which was  
491 characterized to be capable of transfer electrons from acetate to the electrode<sup>60</sup>. Therefore,  
492 the above results strongly implied the AGS close to carbon brush might play more  
493 important role in the electricity generation than the AGS far from carbon brush.

#### 494 **Implications**

495 This study demonstrated the proof concept of using intact AGS as biocatalyst in an MFC  
496 for simultaneous carbon removal and electricity generation. Compared to the conventional  
497 biocatalyst (e.g., domestic wastewater), the AGS has several merits. Firstly, the large  
498 surface area of AGS enabled a substantial electrogenic bacterial growth. Secondly, the  
499 MFC inoculated with AGS generated much higher current compared to the conventional  
500 MFC at same level of substrate. Lastly, the coulombic efficiency improved from 13.62%  
501 (before potential control, 1g/L, 10  $\Omega$ ) to 33.82% (with potential control, 1 g/L) as indicated  
502 in Table S2. Although small improvement, the coulombic losses from methanogenic  
503 process were diminished. The relatively low value (34%) might be due to other process  
504 such as the cathodic oxygen diffusion or competition from other biological species<sup>61, 62</sup>.

505 Meanwhile, it must be pointed out that though AGS contributed the major part of current  
506 generation, the biofilm derived from AGS on the surface of anode electrode is also crucial,  
507 as it might play a role of conduit for electron transfer between bulk AGS and electrode.  
508 The results indicate that it is possible to boost the current generation of MFC by employing  
509 AGS as biocatalyst, but a thin biofilm between ASG and electrode is still needed and may  
510 play an important role to efficiently harvest the energy generated by AGS. The special  
511 conductive property between AGS and the electrode may open up many other intriguing  
512 applications. For instance, the exoelectrogenic AGS could be used as the bed electrodes in  
513 METland (wetland plus MET) and other fluidized bed reactor systems<sup>63</sup>.

514 Furthermore, more efforts should be made to further boost the application of AGS for  
515 energy recovery and simultaneous wastewater treatment. For instance, the mechanisms of  
516 electron transfer among granules should be explored to get better understanding of the  
517 system. In that case, how to accelerate the long distance of electron transfer in bacterial  
518 community could be identified and addressed well. Another interesting focus could be the  
519 studying of layer bacterial distribution in the granules and their involvements in the  
520 electron transfer. Further work should also focus on the continuous operation mode and  
521 reactor configuration, for example up flow MFC to optimize the settlement of granules for  
522 the future potential up scaling, or utilizing gas diffusion air cathode to bringing MFC closer  
523 to practical applications<sup>64</sup>.

#### 524 **Supporting Information**

525 Table S1, Figure S1, Figure S2, Figure S3, Figure S4, and Figure S5 as noted in the text.

526 This material is available free of charge via the Internet at <http://pubs.acs.org/>

**527 Author Contributions**

528 YZ, IA and NZ designed the experiments, NZ and LT carried out the research. The  
529 manuscript was written through contributions of all authors. YZ is responsible for  
530 correspondence.

**531 Funding Sources**

532 This research was supported financially by The Danish Council for Independent Research  
533 (DFR-1335-00142) and Novo Nordisk Foundation (NNF16OC0021568).

**534 Acknowledgements**

535 The authors would like to acknowledge China Scholarship Council for the financial  
536 support. The author would also thank the EliteForsk travel funding supported by Danish  
537 Ministry of Education and Research. The authors would also like to acknowledge the  
538 technical assistance by Hector Gracia with analytical measurements, and Aleksandra  
539 Kulagowska and Colsen (The Netherlands) for offering anaerobic granular sludge.

**540 References**

- 541 1. McCarty, P. L.; Bae, J.; Kim, J., Domestic wastewater treatment as a net energy  
542 producer--can this be achieved? *Environ Sci Technol* **2011**, *45*, (17), 7100-7106.
- 543 2. Harnisch, F.; Urban, C., Electrobiorefineries: Unlocking the Synergy of  
544 Electrochemical and Microbial Conversions. *Angew. Chem-International Edition* **2018**, *57*,  
545 (32), 10016-10023.

- 546 3. Liu, H.; Ramnarayanan, R.; Logan, B. E., Production of electricity during  
547 wastewater treatment using a single chamber microbial fuel cell. *Environ Sci Technol* **2004**,  
548 38, (7), 2281-2285.
- 549 4. Min, B.; Logan, B. E., Continuous electricity generation from domestic wastewater  
550 and organic substrates in a flat plate microbial fuel cell. *Environ Sci Technol* **2004**, 38,  
551 (21), 5809-5814.
- 552 5. Ren, L.; Ahn, Y.; Logan, B. E., A Two-Stage Microbial Fuel Cell and Anaerobic  
553 Fluidized Bed Membrane Bioreactor (MFC-AFMBR) System for Effective Domestic  
554 Wastewater Treatment. *Environ Sci Technol* **2014**, 48, (7), 4199-4206.
- 555 6. Wang, Y. K.; Sheng, G. P.; Li, W. W.; Huang, Y. X.; Yu, Y. Y.; Zeng, R. J.; Yu,  
556 H. Q., Development of a novel bioelectrochemical membrane reactor for wastewater  
557 treatment. *Environ Sci Technol* **2011**, 45, (21), 9256-9261.
- 558 7. Lovley, D. R., Bug juice: harvesting electricity with microorganisms. *Nat Rev*  
559 *Microbiol* **2006**, 4, (7), 497-508.
- 560 8. Zhang, Y.; Angelidaki, I., Microbial Electrochemical Systems and Technologies: It  
561 Is Time To Report the Capital Costs. *Environ Sci Technol* **2016**, 50, (11), 5432-5433.
- 562 9. An, J.; Li, N.; Wan, L.; Zhou, L.; Du, Q.; Li, T.; Wang, X., Electric field induced  
563 salt precipitation into activated carbon air-cathode causes power decay in microbial fuel  
564 cells. *Water Res* **2017**, 123, 369-377.
- 565 10. Kosaric, N.; Blaszczyk, R.; Orphan, L.; Valladares, J., The characteristics of  
566 granules from upflow anaerobic sludge blanket reactors. *Water Res* **1990**, 24, (12), 1473-  
567 1477.

- 568 11. Lettinga, G.; Pol, L. W. H., UASB-process design for various types of wastewaters.  
569 *Water Sci Technol* **1991**, 24, (8), 87-107.
- 570 12. Schmidt, J. E.; Ahring, B. K., Granular sludge formation in upflow anaerobic sledge  
571 blanket (UASB) reactors. *Biotechnol Bioeng* **1996**, 49, (3), 229-246.
- 572 13. He, Z.; Minteer, S. D.; Angenent, L. T., Electricity generation from artificial  
573 wastewater using an upflow microbial fuel cell. *Environ Sci Technol* **2005**, 39, (14), 5262-  
574 5267.
- 575 14. Morita, M.; Malvankar, N. S.; Franks, A. E.; Summers, Z. M.; Giloteaux, L.; Rotaru,  
576 A. E.; Rotaru, C.; Lovley, D. R., Potential for Direct Interspecies Electron Transfer in  
577 Methanogenic Wastewater Digester Aggregates. *Mbio* **2011**, 2, (4), 1-8.
- 578 15. Lovley, D. R., Happy together: microbial communities that hook up to swap  
579 electrons. *ISME J* **2017**, 11, (2), 327-336.
- 580 16. Gell, K., Review of Small Scale, Community Biogas in the Industrialized World.  
581 Wageningen University, Netherlands: Community Composting Network. **2008**.
- 582 17. Chong, S.; Sen, T. K.; Kayaalp, A.; Ang, H. M., The performance enhancements of  
583 upflow anaerobic sludge blanket (UASB) reactors for domestic sludge treatment--a state-  
584 of-the-art review. *Water Res* **2012**, 46, (11), 3434-3470.
- 585 18. Zhang, Y.; Angelidaki, I., Recovery of ammonia and sulfate from waste streams  
586 and bioenergy production via bipolar bioelectrodialysis. *Water Res* **2015**, 85, 177-184.
- 587 19. Zhao, N.; Li, X.; Jin, X.; Angelidaki, I.; Zhang, Y., Integrated electrochemical-  
588 biological process as an alternative mean for ammonia monitoring during anaerobic  
589 digestion of organic wastes. *Chemosphere* **2018**, 195, 735-741.

- 590 20. Zhang, Y.; Noori, J. S.; Angelidaki, I., Simultaneous organic carbon, nutrients  
591 removal and energy production in a photomicrobial fuel cell (PFC). *Energy Environ. Sci*  
592 **2011**, 4, (10), 4340-4346.
- 593 21. Jin, X.; Zhang, Y.; Li, X.; Zhao, N.; Angelidaki, I., Microbial Electrolytic Capture,  
594 Separation and Regeneration of CO<sub>2</sub> for Biogas Upgrading. *Environ Sci Technol* **2017**, 51,  
595 (16), 9371-9378.
- 596 22. Zhao, N.; Angelidaki, I.; Zhang, Y., Electricity generation and microbial  
597 community in response to short-term changes in stack connection of self-stacked  
598 submersible microbial fuel cell powered by glycerol. *Water Res* **2017**, 109, 367-374.
- 599 23. Zhao, N.; Jiang, Y.; Alvarado-Morales, M.; Treu, L.; Angelidaki, I.; Zhang, Y.,  
600 Electricity generation and microbial communities in microbial fuel cell powered by  
601 macroalgal biomass. *Bioelectrochemistry* **2018**, 123, 145-149.
- 602 24. Parks, D. H.; Tyson, G. W.; Hugenholtz, P.; Beiko, R. G., STAMP: statistical  
603 analysis of taxonomic and functional profiles. *Bioinformatics* **2014**, 30, (21), 3123-3124.
- 604 25. Jadhav, G. S.; Ghangrekar, M. M., Performance of microbial fuel cell subjected to  
605 variation in pH, temperature, external load and substrate concentration. *Bioresour Technol*  
606 **2009**, 100, (2), 717-723.
- 607 26. Ren, Z.; Yan, H.; Wang, W.; Mench, M. M.; Regan, J. M., Characterization of  
608 Microbial Fuel Cells at Microbially and Electrochemically Meaningful Time scales.  
609 *Environ Sci Technol* **2011**, 45, (6), 2435-2441.

- 610 27. Song, T.-S.; Yan, Z.-S.; Zhao, Z.-W.; Jiang, H.-L., Removal of organic matter in  
611 freshwater sediment by microbial fuel cells at various external resistances. *J Chem Technol*  
612 *Biotechnol* **2010**, 1489-1493.
- 613 28. Jung, S.; Regan, J. M., Influence of external resistance on electrogenesis,  
614 methanogenesis, and anode prokaryotic communities in microbial fuel cells. *Appl Environ*  
615 *Microbiol* **2011**, 77, (2), 564-571.
- 616 29. Butti, S. K.; Velvizhi, G.; Sulonen, M. L. K.; Haavisto, J. M.; Oguz Koroglu, E.;  
617 Yusuf Cetinkaya, A.; Singh, S.; Arya, D.; Annie Modestra, J.; Vamsi Krishna, K.; Verma,  
618 A.; Ozkaya, B.; Lakaniemi, A.-M.; Puhakka, J. A.; Venkata Mohan, S., Microbial  
619 electrochemical technologies with the perspective of harnessing bioenergy: Maneuvering  
620 towards upscaling. *Renew Sust Energ Rev* **2016**, 53, 462-476.
- 621 30. Rotaru, A.-E.; Shrestha, P. M.; Liu, F.; Shrestha, M.; Shrestha, D.; Embree, M.;  
622 Zengler, K.; Wardman, C.; Nevin, K. P.; Lovley, D. R., A new model for electron flow  
623 during anaerobic digestion: direct interspecies electron transfer to Methanosaeta for the  
624 reduction of carbon dioxide to methane. *Energy Environ. Sci* **2014**, 7, (1), 408-415.
- 625 31. Sleutels, T. H.; Molenaar, S. D.; Heijne, A. T.; Buisman, C. J., Low Substrate  
626 Loading Limits Methanogenesis and Leads to High Coulombic Efficiency in  
627 Bioelectrochemical Systems. *Microorganisms* **2016**, 4, (1), 1-11.
- 628 32. Logan, B. E., Exoelectrogenic bacteria that power microbial fuel cells. *Nat Rev*  
629 *Microbiol* **2009**, 7, (5), 375-381.
- 630 33. Schroder, U., Anodic electron transfer mechanisms in microbial fuel cells and their  
631 energy efficiency. *Phys Chem Chem Phys* **2007**, 9, (21), 2619-2629.

- 632 34. Hari, A. R.; Katuri, K. P.; Logan, B. E.; Saikaly, P. E., Set anode potentials affect  
633 the electron fluxes and microbial community structure in propionate-fed microbial  
634 electrolysis cells. *Sci Rep* **2016**, 6, 38690.
- 635 35. Carmona-Martinez, A. A.; Harnisch, F.; Kuhlicke, U.; Neu, T. R.; Schroder, U.,  
636 Electron transfer and biofilm formation of *Shewanella putrefaciens* as function of anode  
637 potential. *Bioelectrochemistry* **2013**, 93, 23-29.
- 638 36. Logan, B. E.; Regan, J. M., Electricity-producing bacterial communities in  
639 microbial fuel cells. . *Trends Microbiol* **2006**, 14, (12), 512-518.
- 640 37. Ren, Z.; Steinberg, L. M.; Regan, J. M., Electricity production and microbial  
641 biofilm characterization in cellulose-fed microbial fuel cells. *Water Sci Technol* **2008**, 58,  
642 (3), 617.
- 643 38. Margaria, V.; Tommasi, T.; Pentassuglia, S.; Agostino, V.; Sacco, A.; Armato, C.;  
644 Chiodoni, A.; Schilirò, T.; Quaglio, M., Effects of pH variations on anodic marine consortia  
645 in a dual chamber microbial fuel cell. *Int J Hydrog Energy* **2017**, 42, (3), 1820-1829.
- 646 39. Pevere, A.; Guibaud, G.; Goin, E.; van Hullebusch, E.; Lens, P., Effects of physico-  
647 chemical factors on the viscosity evolution of anaerobic granular sludge. *Biochem Eng J*  
648 **2009**, 43, (3), 231-238.
- 649 40. Quarmby, J.; Forster, C. F., A comparative study of the internal architecture of  
650 anaerobic granular sludges. *J Chem Technol Biotechnol* **1995**, 63, (1), 60-68.
- 651 41. Diaz, E. E.; Stams, A. J.; Amils, R.; Sanz, J. L., Phenotypic properties and microbial  
652 diversity of methanogenic granules from a full-scale upflow anaerobic sludge bed reactor  
653 treating brewery wastewater. *Appl Environ Microbiol* **2006**, 72, (7), 4942-4949.



- 654 42. Kuznar, Z. A.; Elimelech, M., Adhesion kinetics of viable *Cryptosporidium parvum*  
655 oocysts to quartz surfaces. *Environ Sci Technol* **2004**, 38, (24), 6839-6845.
- 656 43. De Kerchove, A. J.; Elimelech, M., Calcium and magnesium cations enhance the  
657 adhesion of motile and nonmotile *Pseudomonas aeruginosa* on alginate films. *Langmuir*  
658 **2008**, 24, (7), 3392-3399.
- 659 44. Harris, H. W.; El-Naggar, M. Y.; Bretschger, O.; Ward, M. J.; Romine, M. F.;  
660 Obraztsova, A. Y.; Nealson, K. H., Electrokinesis is a microbial behavior that requires  
661 extracellular electron transport. *Proc Natl Acad Sci USA* **2010**, 107, (1), 326-331.
- 662 45. Zhu, X.; Treu, L.; Kougias, P. G.; Campanaro, S.; Angelidaki, I., Characterization  
663 of the planktonic microbiome in upflow anaerobic sludge blanket reactors during  
664 adaptation of mesophilic methanogenic granules to thermophilic operational conditions.  
665 *Anaerobe* **2017**, 46, 69-77.
- 666 46. Zhang, Y.; Wang, Y.; Angelidaki, I., Alternate switching between microbial fuel  
667 cell and microbial electrolysis cell operation as a new method to control H<sub>2</sub>O<sub>2</sub> level in  
668 Bioelectro-Fenton system. *J Power Sources* **2015**, 291, 108-116.
- 669 47. Borole, A. P.; Hamilton, C. Y.; Vishnivetskaya, T. A., Enhancement in current  
670 density and energy conversion efficiency of 3-dimensional MFC anodes using pre-enriched  
671 consortium and continuous supply of electron donors. *Bioresour Technol* **2011**, 102, (8),  
672 5098-5104.
- 673 48. Fedorovich, V.; Knighton, M. C.; Pagaling, E.; Ward, F. B.; Free, A.; Goryanin, I.,  
674 Novel Electrochemically Active Bacterium Phylogenetically Related to *Arcobacter*

- 675 butzleri, Isolated from a Microbial Fuel Cell. *Appl. Environ. Microbiol.* **2009**, 75, (23),  
676 7326-7334.
- 677 49. Liu, L.; Tsyganova, O.; Lee, D.-J.; Chang, J.-S.; Wang, A.; Ren, N., Double-  
678 chamber microbial fuel cells started up under room and low temperatures. *Int J Hydrog*  
679 *Energy* **2013**, 38, (35), 15574-15579.
- 680 50. Sotres, A.; Tey, L.; Bonmati, A.; Vinas, M., Microbial community dynamics in  
681 continuous microbial fuel cells fed with synthetic wastewater and pig slurry.  
682 *Bioelectrochemistry* **2016**, 111, 70-82.
- 683 51. Ma, K.; Liu, X. L.; Dong, X. Z., Methanobacterium beijingense sp nov., a novel  
684 methanogen isolated from anaerobic digesters. *Int J Syst Evol Microbiol* **2005**, 55, 325-329.
- 685 52. Gagliano, M. C.; Ismail, S. B.; Stams, A. J. M.; Plugge, C. M.; Temmink, H.; Van  
686 Lier, J. B., Biofilm formation and granule properties in anaerobic digestion at high salinity.  
687 *Water Res* **2017**, 121, 61-71.
- 688 53. Kiely, P. D.; Regan, J. M.; Logan, B. E., The electric picnic: synergistic  
689 requirements for exoelectrogenic microbial communities. *Curr Opin Biotechnol* **2011**, 22,  
690 (3), 378-385.
- 691 54. Logan, B. E.; Rossi, R.; Ragab, A.; Saikaly, P. E., Electroactive microorganisms in  
692 bioelectrochemical systems. *Nat Rev Microbiol* **2019**, 17, (5), 307-319.
- 693 55. Chae, K. J.; Choi, M. J.; Lee, J. W.; Kim, K. Y.; Kim, I. S., Effect of different  
694 substrates on the performance, bacterial diversity, and bacterial viability in microbial fuel  
695 cells. *Bioresour Technol* **2009**, 100, (14), 3518-3525.

- 696 56. Ahlert, S.; Zimmermann, R.; Ebling, J.; König, H., Analysis of propionate-  
697 degrading consortia from agricultural biogas plants. *Microbiologyopen* **2016**, 5, (6), 1027-  
698 1037.
- 699 57. Lange, M.; Ahring, B. K., A comprehensive study into the molecular methodology  
700 and molecular biology of methanogenic Archaea. *Fems Microbiol Rev* **2001**, 25, (5), 553-  
701 571.
- 702 58. Mateos, R.; Escapa, A.; San-Martín, M. I.; Wever, H. D.; Sotres, A.; Pant, D., Long-  
703 term open circuit microbial electrosynthesis system promotes methanogenesis. *J Eng Chem*  
704 **2020**, 41, 3-6.
- 705 59. Jadhav, D. A.; Chendake, A. D.; Schievano, A.; Pant, D., Suppressing methanogens  
706 and enriching electrogens in bioelectrochemical systems. *Bioresour Technol* **2019**, 277,  
707 148-156.
- 708 60. Toh, H.; Sharma, V. K.; Oshima, K.; Kondo, S.; Hattori, M.; Ward, F. B.; Free, A.;  
709 Taylor, T. D., Complete genome sequences of *Arcobacter butzleri* ED-1 and *Arcobacter*  
710 sp. strain L, both isolated from a microbial fuel cell. *J Bacteriol* **2011**, 193, (22), 6411-  
711 6412.
- 712 61. Ahn, Y.; Logan, B. E., Domestic wastewater treatment using multi-electrode  
713 continuous flow MFCs with a separator electrode assembly design. *Appl Microbiol*  
714 *Biotechnol* **2013**, 97, (1), 409-416.
- 715 62. Kim, K. Y.; Yang, W.; Logan, B. E., Impact of electrode configurations on retention  
716 time and domestic wastewater treatment efficiency using microbial fuel cells. *Water Res*  
717 **2015**, 80, 41-46.

718 63. Ramírez-Vargas, C.; Prado, A.; Arias, C.; Carvalho, P.; Esteve-Núñez, A.; Brix,  
719 H., Microbial Electrochemical Technologies for Wastewater Treatment: Principles and  
720 Evolution from Microbial Fuel Cells to Bioelectrochemical-Based Constructed Wetlands.  
721 *Water* **2018**, 10, (9).

722 64. Rossi, R.; Jones, D.; Myung, J.; Zikmund, E.; Yang, W.; Gallego, Y. A.; Pant, D.;  
723 Evans, P. J.; Page, M. A.; Cropek, D. M.; Logan, B. E., Evaluating a multi-panel air cathode  
724 through electrochemical and biotic tests. *Water Res* **2019**, 148, 51-59.

725

726 **List of figure captions**

727 Figure 1 Current density (A), TCOD removal (B) and biogas production rate and methane  
728 yield (C) over time at different external resistance and different acetate concentrations. Red  
729 line and green line refer to the performance of R-10 ohm, 1500 mg/L in Strategy 1 and  
730 Strategy 2, respectively.

731 Figure 2 Current density (A), acetate concentrations (B) and average biogas production rate  
732 and methane yield (C) with time in different reactors. Control 1: MFC with only carbon  
733 brush (after potential control and moving granules out).

734 Figure 3 The maximum current density and COD removal rate coefficient at varied pH  
735 conditions. AGS-MFC: MFC after potential control; Control 3: MFC inoculated with  
736 domestic wastewater.

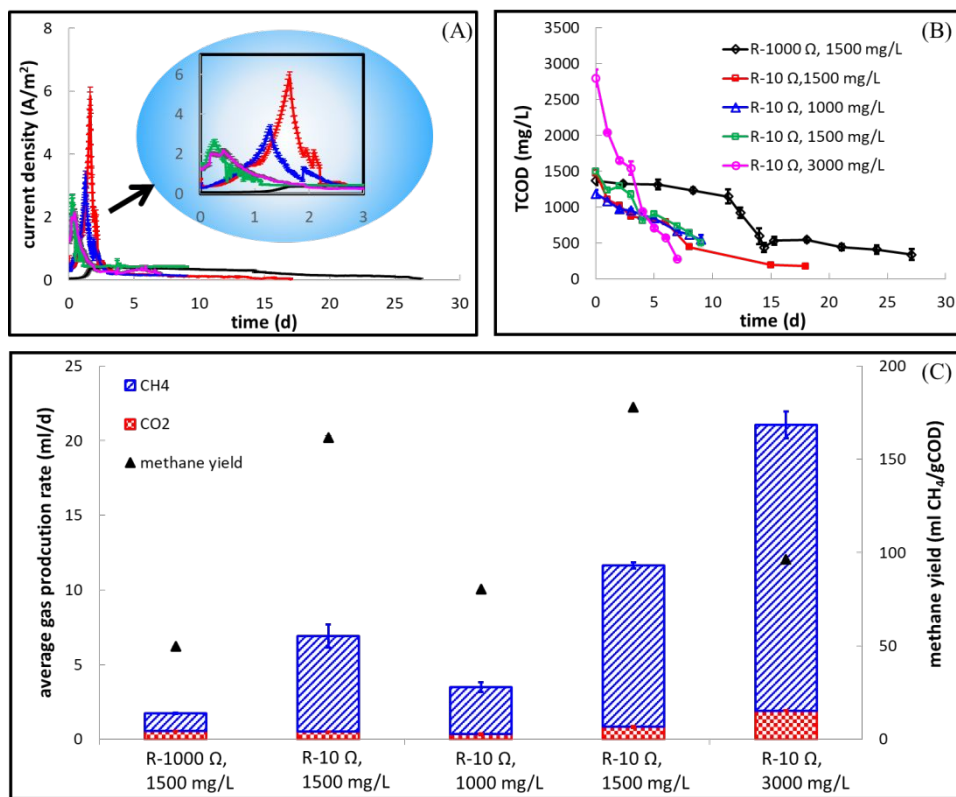
737 Figure 4 SEM image of the surface structure of single GAS after anodic potential  
738 control:(A) an intact granule; (B) high-resolution of SEM image of granular surface  
739 showing the massive microbial colonization; (C) showing the rod-shape microbes aligned  
740 on the side of deep channels. (D) Energy-dispersive X-ray (EDS) results of AGS before  
741 and after strategy 3. (E) Particle size distribution of raw AGS and cultivated AGS after  
742 strategy 3.

743 Figure 5 Microbial community compositions in raw AGS (G1), and enriched AGS after  
744 anode potential control and close to carbon brush (G2), enriched AGS far from carbon  
745 brush (G3), and biofilm on carbon brush (Biofilm). Relative abundance (%) and folds  
746 change were reported in (A) and (B), respectively. Group 1: the taxa increased in relative

747 abundance after anode potential control. Group 2: the taxa decreased in relative abundance  
748 after anode potential control.

749 Figure 6 OTUs that changed significantly ( $p < 0.05$ ) in the comparison between G2  
750 (enriched AGS taken from close to carbon brush after strategy 3) and Biofilm (A), between  
751 G3 (enriched AGS taken far from carbon brush after strategy 3) and Biofilm (B), and  
752 between G3 and G2 (C), respectively.

753



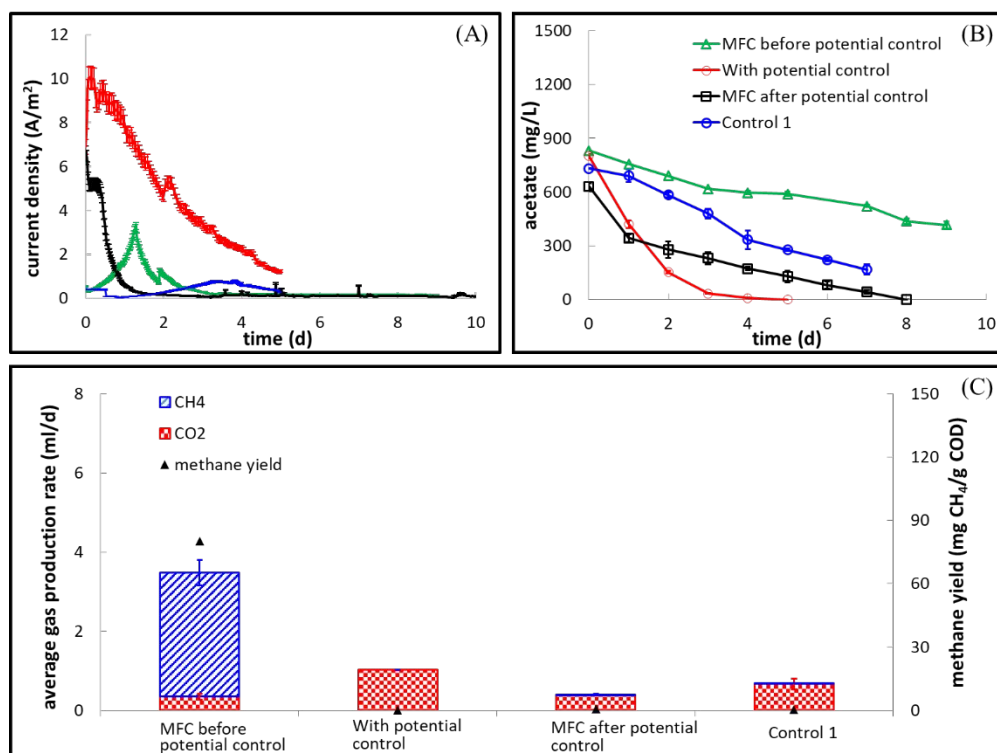
754

755

756

Figure 1

757



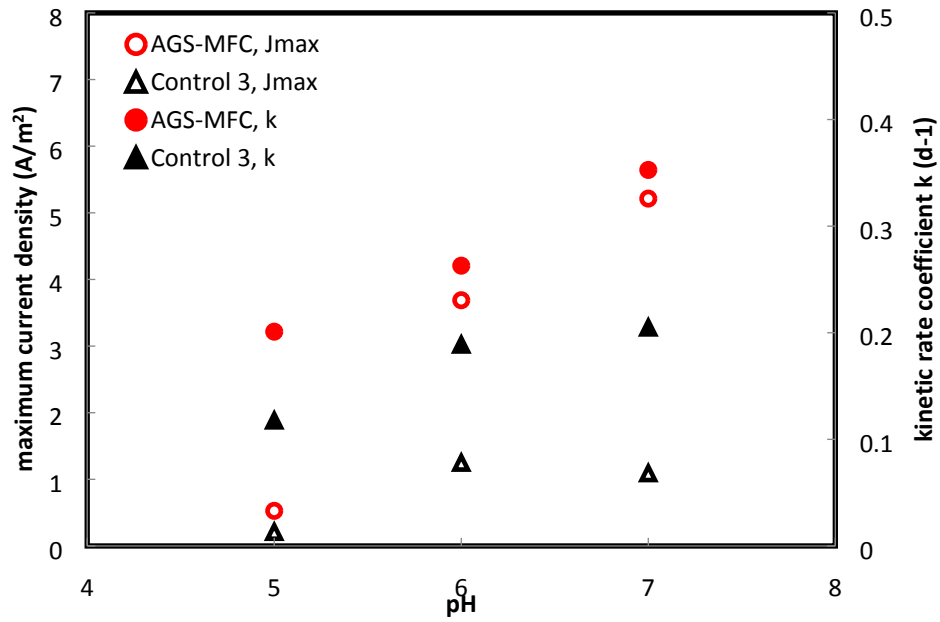
758

759

Figure 2

760





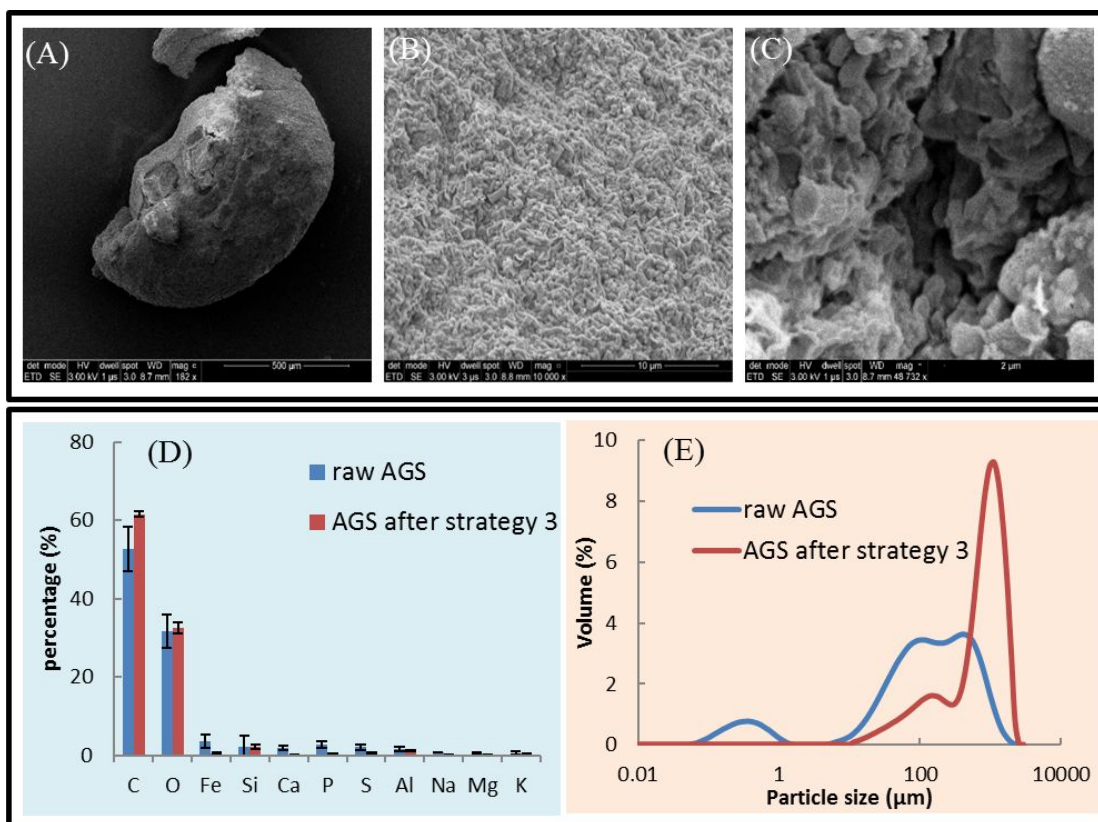
761

762

763

764

Figure 3

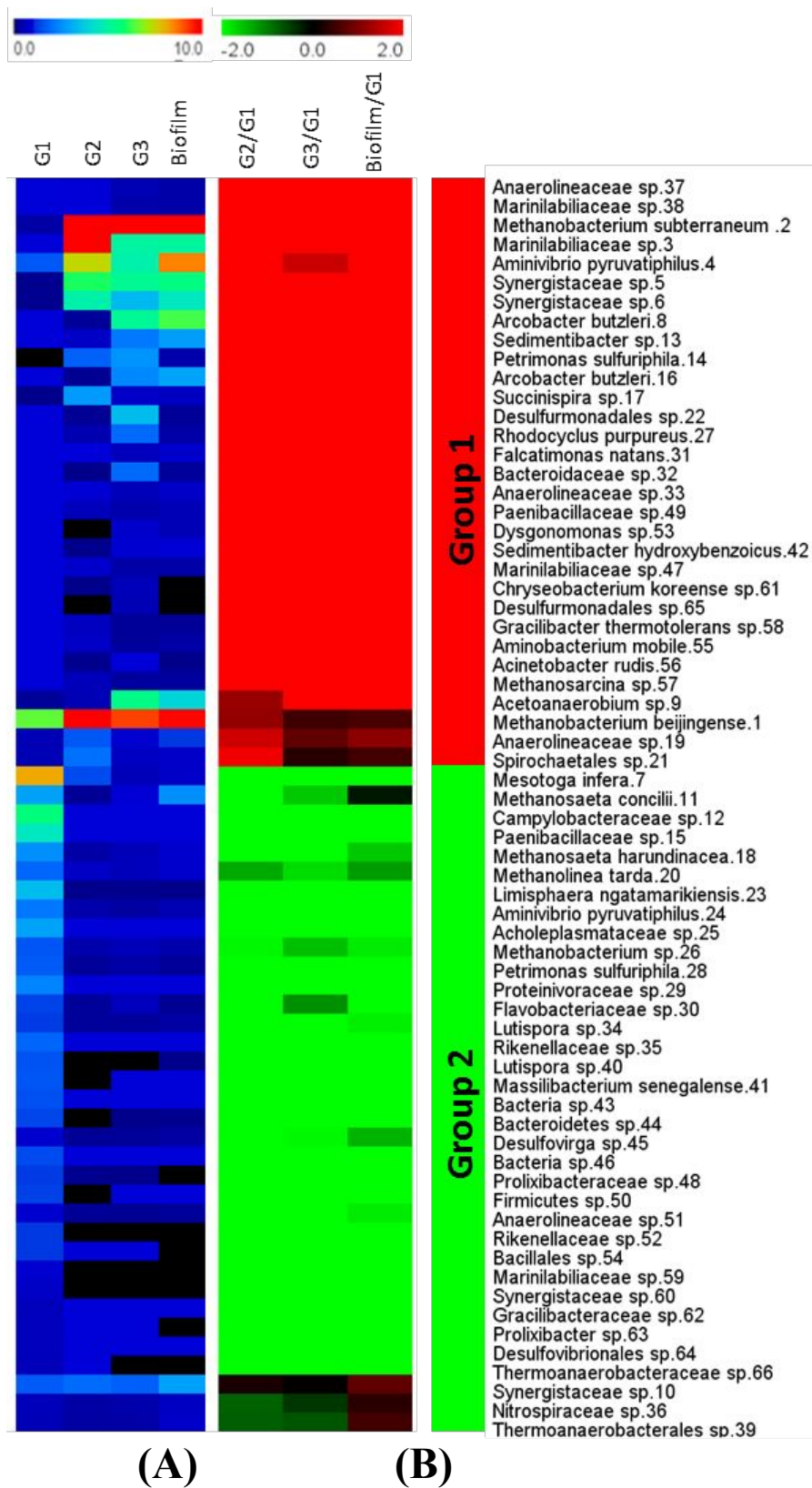


765

766

767

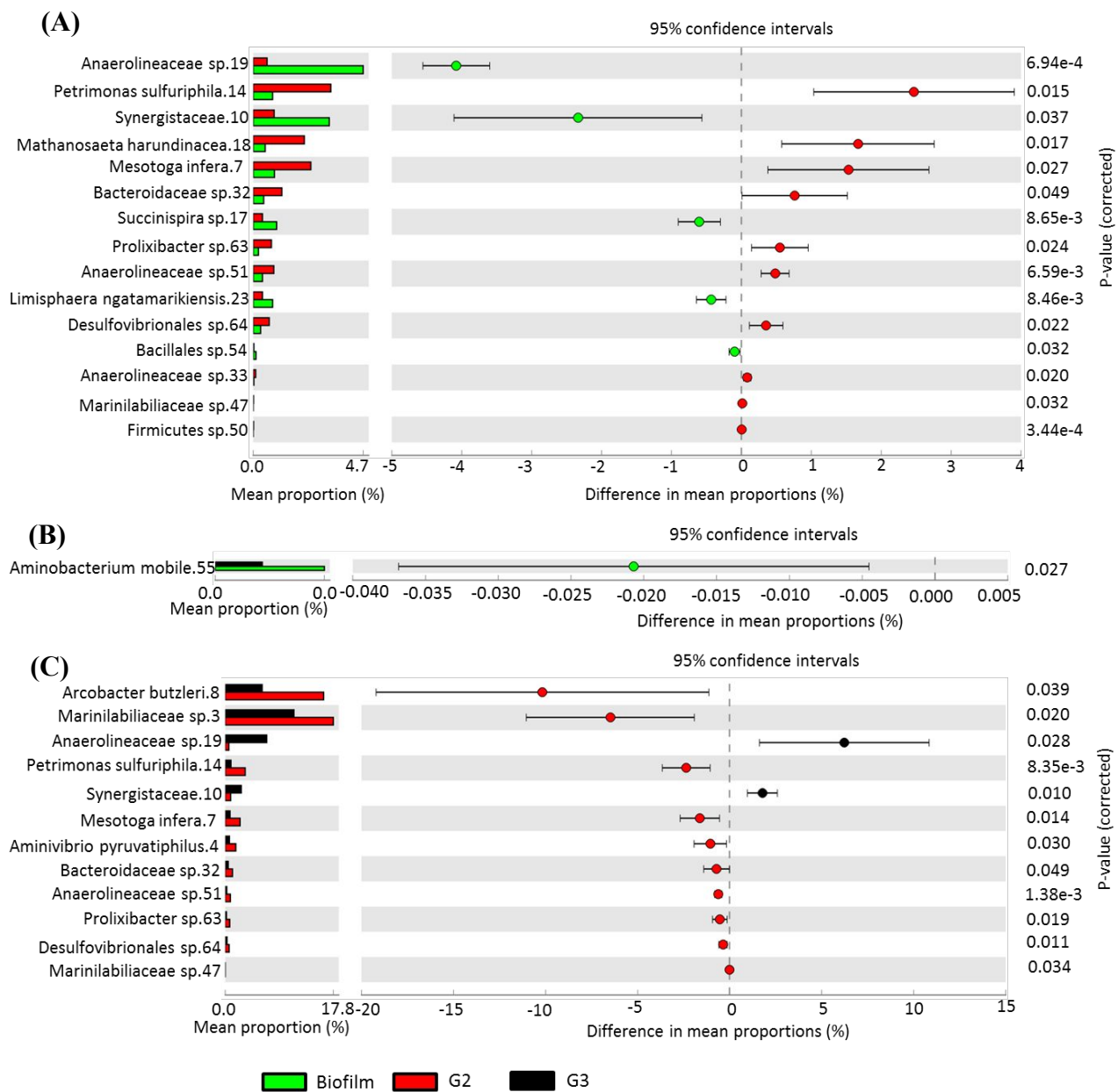
Figure 4



768

769

Figure 5



770

771

772

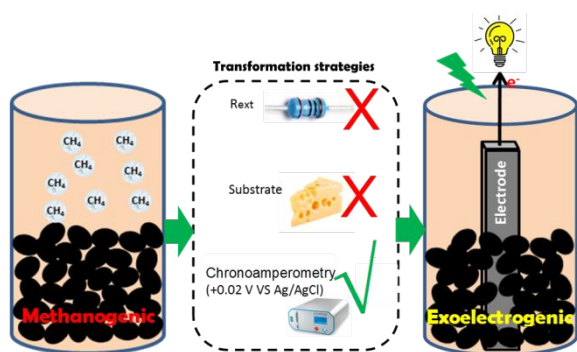
773

774

775

Figure 6

## 776 TOC Art



777

778